
From PEFT to DEFT: Parameter Efficient Finetuning for Reducing Activation Density in Transformers

Bharat Runwal¹ Tejaswini Pedapati² Pin-Yu Chen²

Abstract

Pretrained Language Models (PLMs) have become the de facto starting point for fine-tuning on downstream tasks. However, as model sizes continue to increase, traditional fine-tuning of all parameters becomes challenging. To address this, parameter-efficient fine-tuning (PEFT) methods have gained popularity as a means to adapt PLMs effectively. In parallel, recent studies have revealed the presence of activation sparsity within the intermediate outputs of the multilayer perception (MLP) blocks in transformers. Low activation density enables efficient model inference on sparsity-aware hardware. Building upon this insight, in this work, we propose a novel density loss that encourages higher activation sparsity (equivalently, lower activation density) in the pre-trained models. We demonstrate the effectiveness of our approach by utilizing mainstream PEFT techniques including QLoRA, LoRA, Adapter, Prompt/Prefix Tuning to facilitate efficient model adaptation across diverse downstream tasks. Experiments show that our proposed method DEFT, Density-Efficient Fine-Tuning, can reduce the activation density consistently and up to **50.72%** on RoBERTa_{Large}, and **53.19%** (encoder density) and **90.60%** (decoder density) on Flan-T5_{XXL} (**11B**) compared to PEFT using GLUE and QA (SQuAD) benchmarks respectively while maintaining competitive performance on downstream tasks. We also showcase that DEFT works complementary with quantized and pruned models.¹

1. Introduction

With the advent of pre-trained large language models (LLMs) (Devlin et al., 2019; Radford et al., 2019b; Raffel et al., 2020), fine-tuning (Howard & Ruder, 2018) these

¹Independent Researcher ²IBM Research. Correspondence to: Bharat Runwal <bharatrunwal@gmail.com>.

Preprint Under Review. Copyright 2024 by the author(s).

¹Our Code can be accessed at <https://github.com/IBM/DEFT>

models to adapt to a task has become prevalent. However, training these models and performing inference on them requires a significant amount of time, energy, and memory, thereby resulting in an enormous carbon footprint (Strubell et al., 2019). Some methods to achieve faster and greener inference are by pruning the model parameters (Lee et al., 2019; Tanaka et al., 2020), pruning the number of heads by analyzing the attention patterns in the heads (Behnke & Heafield, 2020; Voita et al., 2019; Michel et al., 2019), distilling the larger model to a smaller model (Sanh et al., 2019), quantizing the models to convert the weights to a lower precision (Dettmers et al., 2022; Zadeh et al., 2020), using mixture of experts (MOE) (Kudugunta et al., 2021; Rajbhandari et al., 2022), etc. In contrast to all these techniques, this paper focuses on accelerating the model inference by increasing the activation sparsity in the model. This is achieved by including a penalty for high activation density in the loss function.

Recent studies (Zhang et al., 2021; Li et al., 2022) have shown that in a transformer architecture, specifically in the intermediate outputs of MLP (Multi-Layer Perceptron) blocks with ReLU activations, only a fraction of neurons are activated for a given input, leading to the sparse activation maps as the output. Building upon this observation, we propose a novel density loss that encourages higher activation sparsity in pre-trained models when adapting to downstream tasks, effectively reducing the activation density.

Moreover, the induction of higher activation sparsity holds promising prospects for substantial energy savings, especially on modern hardware acceleration architectures like ASICs (Application Specific Integrated Circuits) (Lazzaro et al., 2023), which leverage zero-skip operations. By promoting sparsity in the activation maps of transformers, hardware can take advantage of zero-skip operations, skipping unnecessary computations on zero-valued activations, resulting in reduced power consumption and more efficient model inference. This energy-efficient approach becomes particularly advantageous for resource-constrained environments or applications with strict energy constraints.

In this work, we present Density-Efficient Fine-Tuning (DEFT), which induces activation sparsity using parameter-efficient fine-tuning (PEFT) techniques. We illustrate our

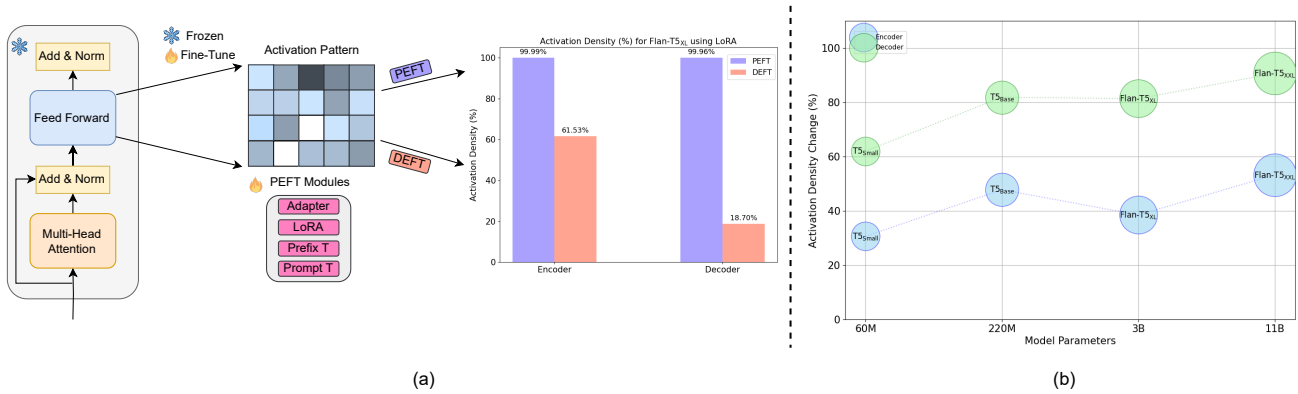


Figure 1: (a) Comparison between the activation density (in the intermediate output of MLP) after adapting to downstream tasks with PEFT and our proposed DEFT method. Both methods use LoRA. (b) Activation Density Change (%) of DEFT relative to PEFT for different scales of the T5 encoder-decoder model family on SQuAD dataset (Rajpurkar et al., 2016). Both methods use LoRA.

proposed method DEFT in Figure (1a), and the histogram plot shows the reduction in Activation Density (%), which is defined as the number of non-zero values in the intermediate output of MLP layers in transformer blocks averaged over the full validation set. Our proposed method DEFT significantly lowers the activation density compared to PEFT. Figure (1b) further illustrates the change in activation density (as formally defined in Eq. (8)) with DEFT relative to PEFT in scaling T5-family models using the LoRA module. Notably, our method induces sparser activation patterns, which become even more pronounced with increasing model size. Higher Density Change (%) is indicative of a greater reduction in activation density compared to PEFT. This means that DEFT not only leads to sparser activation patterns than PEFT but also shows that as the model size increases, the activation patterns become increasingly sparse. This trend underscores the scalability of DEFT’s effectiveness in reducing activation density with larger model sizes.

To the best of our knowledge, we are the first to demonstrate that a significant degree of activation sparsity can be attained using a small number of trainable parameters. This is particularly notable in GeLU (Hendrycks & Gimpel, 2016) models (GeLU is the default activation function of state-of-the-art transformer models). Prior studies primarily concentrated on ReLU-based models for investigating activation sparsity (Lazzaro et al., 2023), which are known for their inherent sparsity in activation maps. Our approach, combining PEFT and activation sparsity, paves the way for resource-friendly transformer models across various applications.

2. Related Work

2.1. Weight Induced Sparsity

Reducing the number of parameters of the model results in a model with lesser memory footprint, reducing the amount of computational resources required to perform the infer-

ence. This can be done by pruning those parameters of the model whose removal does not deteriorate the model’s performance significantly. To prune the weights at initialization using unstructured pruning, methods such as snip (Lee et al., 2019), grasp (Wang et al., 2020), synaptic flow (Tanaka et al., 2020), etc can be leveraged.

Prior arts such as (Li et al., 2021; Voita et al., 2019; Michel et al., 2019; Behnke & Heafield, 2020) sort the heads based on various importance scores and prune the bottom rung. For instance, in the case of (Michel et al., 2019), the importance score is the difference in loss values of when the head is not pruned and when it is pruned. Both (Voita et al., 2019) and (Behnke & Heafield, 2020) use the confidence of heads as the pruning metric.

Distilling the original model into a smaller model with fewer parameters also achieves the same goal. DistilBert (Sanh et al., 2019) was obtained by using knowledge distillation on the BERT model during the pre-training phase and is 40% smaller than BERT while being 97% as performant as BERT.

(Chen et al., 2021) used a parameter efficient fine-tuning technique that performs low rank weight updates similar to LoRA. The user inputs the desired sparsity and whether entire heads must be pruned or any model parameters can be pruned. After training, the model parameters and the heads are sorted by the gradient magnitude and are pruned according to the user’s preference to achieve the desired sparsity. The importance score for pruning the model parameters in (Sun et al., 2023a) is a product of the magnitude of the weights and the norm of the input’s activations.

2.2. Activation Induced Sparsity

Rather than eliminating the parameters apriori, inducing activation sparsity dynamically reduces the latency on a sparsity-aware hardware by reducing the number of computations. (Li et al., 2022) demonstrated that the larger the

language models, the sparser their layer outputs are. Although the output was sparse, there was never a neuron that was never activated. While 93.5% of the neurons were activated less than 10% of the time, the least activated neuron was fired at least 0.001% of the time. Activation sparsity is achieved by thresholding the top-k activation outputs and zeroing out the rest.

(Kurtz et al., 2020) modified ReLU activation of ResNet18 models to fire only if the magnitude of the input is higher than the specified threshold. They developed special sparsity aware convolution algorithm to accelerate inference. As opposed to this, our method naturally induces the activation sparsity during the training owing to our loss function.

3. Methodology

3.1. Background and Notations

In transformers, the position-wise feed-forward networks employ a two-layer MLP. We measure the activation sparsity at the intermediate output of this two-layer MLP, following the works of (Li et al., 2022) and (Zhang et al., 2021).

Consider an input $X \in \mathbb{R}^{B \times K \times d_{\text{model}}}$, where B is the batch size, K is the sequence length and d_{model} denotes the dimensionality of the input features. Given an input matrix X , the output of the two-layer MLP can be described as:

$$Y(X; W^{(1)}, W^{(2)}) = f(XW^{(1)})W^{(2)} \quad (1)$$

Here $W^{(1)} \in \mathbb{R}^{d_{\text{model}} \times d_{\text{ff}}}$ and $W^{(2)} \in \mathbb{R}^{d_{\text{ff}} \times d_{\text{model}}}$ are the learnable parameters of the MLP layers. d_{ff} represents the hidden dimension of the MLP block, and f is the non-linear activation function.

To measure the sparsity of neuron activations, we first define the activation pattern as :

$$O = f(XW^{(1)}) \quad (2)$$

The matrix $O \in \mathbb{R}^{B \times K \times d_{\text{ff}}}$ is the activation pattern. Following (Li et al., 2022), we can define the vector $s \in \mathbb{R}^{d_{\text{ff}}}$ as the average across the batches and sequence length of matrix O to represents the final feature map. So, we can measure the sparsity of neurons by counting the number of non-zeros in the feature map s .

3.2. Density Loss

In this section, we introduce our proposed Density loss in DEFT. Our goal is to reduce the activation density (or increase activation sparsity) in MLP blocks for given inputs.

Previous work by (Li et al., 2022) used a step function to count the number of positive elements precisely, but this operation is non-differentiable and cannot be used for our pur-

pose of reducing activation density in an end-to-end learning setup. Therefore, to approximate the number of non-zero entries in the sparse vector s , we use the hyperbolic tangent function with a scaling parameter β for ReLU-activation based models as defined in (3) for an input feature x with n elements $\{x_i\}_{i=1}^n$. (Krithivasan et al., 2020) used a similar function for their purpose of generating adversarial inputs for sparsity attacks. We also use a differentiable approximation of the l_0 norm (Lazzaro et al., 2023) for GeLU and other models with activations different from GeLU and ReLU, as defined (4) with some hyperparameter $\epsilon > 0$.

$$\tanh(x, \beta) = \frac{e^{\beta \cdot x} - e^{-\beta \cdot x}}{e^{\beta \cdot x} + e^{-\beta \cdot x}} \quad (3)$$

$$\hat{l}_0(x, \epsilon) = \sum_{i=1}^n \left(\frac{x_i^2}{x_i^2 + \epsilon} \right) \quad (4)$$

By adjusting the value of β in (3), we can control the abruptness to approximate the step function (and therefore sparsity) of the values. Higher values of β make the function more closely resemble the step function. In (4), $\epsilon \in \mathbb{R}$ is a parameter dictating the quality of the approximation—lower values of ϵ correspond to better approximations. We also explore other approximation methods in Appendix A.3.1.

We define the density loss $\mathcal{L}_{\text{density}}(x)$ as follows:

$$\mathcal{L}_{\text{density}}(x) = \frac{1}{n} \sum_{l=1}^L \sum_i g(s_{l_i}) \quad (5)$$

Here, n is the total number of neurons in all the MLP layers, L is the total number of layers in the transformer, and s_l is the feature map after the first dense layer in MLP layer l , with i indexing each feature of s_l . The summation is across all the layers and the elements of the vector s_l . The approximation function g can either be the tanh function (3) or the l_0 approximation (4).

3.3. Parameter Efficient Fine-tuning (PEFT)

Fine-tuning a large language model is computationally expensive, as it involves training all the parameters of the model from scratch. When adapting a model to multiple datasets, the traditional fine-tuning approach necessitates saving all the trained parameters separately for each dataset, leading to significant storage overhead and computational burden. PEFT addresses this by introducing fewer additional trainable parameters. During fine-tuning, only these parameters are trained, with the rest of the model remaining unchanged. This approach not only reduces computational burden but also minimizes storage demands, as only the new parameters need saving, streamlining the model adaptation process.

Our proposed method DEFT is fully compatible with PEFT and in this paper it adopts Prompt tuning (Lester et al., 2021),

Prefix tuning (Li & Liang, 2021), adapters (Houlsby et al., 2019) and Low-rank adaptation (LoRA) (Hu et al., 2022; Dettmers et al., 2023a) techniques for demonstration. Each of these techniques are elaborated in detail in Appendix A.1.

3.4. DEFT: Parameter and Activation Density Efficient Fine-tuning

In our DEFT framework, to efficiently adapt the model without fine-tuning all parameters, we freeze the transformer parameters and only train the aforementioned PEFT modules for downstream tasks.

For PEFT, we solve the following optimization problem:

$$\arg \min_{\Phi} \mathcal{L}_T(D; \{\Theta, \Phi\}) \quad (6)$$

Here, Φ represents a set of additional parameters (tunable) in PEFT, while Θ denotes the set of pre-trained parameters (frozen). The loss function \mathcal{L}_T encapsulates the task-specific objectives and D is the dataset associated with the task.

For our proposed density-efficient fine-tuning (DEFT), i.e. inducing activation sparsity in the MLP layer of transformer blocks, we augment the optimization problem (6) by incorporating our density loss (5):

$$\arg \min_{\Phi} \mathcal{L}_{\text{total}} = \mathcal{L}_T(D; \{\Theta, \Phi\}) + \alpha \cdot \mathcal{L}_{\text{density}}(D; \{\Theta, \Phi\}) \quad (7)$$

Here, the parameter α controls the balance between optimizing the performance metric and inducing activation sparsity. Notably, higher values of α promote sparser activation maps, although a careful equilibrium is required to ensure minimal impact on performance. We have described the algorithm for DEFT in Algorithm 1.

Importantly, the tunable parameters Φ encompass a versatile range of modules, or compositions thereof, from the choice of {Adapters, LoRA, QLoRA, Prefix-Tuning, Prompt-Tuning}, while the original pre-trained parameters Θ remains frozen. We advocate for these parameter-efficient modules over full-finetuning due to our experimental findings, which reveal that the introduction of a small fraction of trainable parameters (just a few % of the full model size) suffices to trigger activation sparsity within the MLP blocks. By incorporating these modules, we achieve a twofold efficiency advantage: (1) Facilitating activation sparsity, primed for utilization by hardware accelerators such as ASIC; and (2) Efficient training and storage of these modules, yielding gains in both training time and memory utilization, all while preserving the integrity of downstream task performance.

4. Experiments

Datasets: We evaluated the performance of our method and PEFT techniques using two benchmark datasets: GLUE

Algorithm 1 DEFT

Require: Dataset D , # of Epochs E , Batch Size B , # of transformer blocks L , Tunable parameters Φ , Coefficient α , Sparsity approximation function g

- 1: **for** epoch $\leftarrow 1$ to E **do**
- 2: **for** batch $\leftarrow 1$ to $\text{length}(D)$ with batch size B **do**
- 3: auxiliary variable $\eta \leftarrow []$
- 4: **for** $i \leftarrow 1$ to L **do**
- 5: $O_i \leftarrow$ Get the intermediate output for MLP $_i$
- 6: $\eta.append(g(O_i))$
- 7: **end for**
- 8: Density Loss: $\mathcal{L}_{\text{density}} \leftarrow \text{mean}(\eta)$
- 9: Total Loss : $\mathcal{L}_{\text{total}} \leftarrow \mathcal{L}_T + \alpha \cdot \mathcal{L}_{\text{density}}$
- 10: Update parameters Φ using $\mathcal{L}_{\text{total}}$ loss
- 11: **end for**
- 12: **end for**

(Wang et al., 2018) and SQuAD (Rajpurkar et al., 2016). We also evaluated our method on CIFAR-10 (Krizhevsky et al., 2009) Dataset in Appendix A.3.4.

The GLUE benchmark comprises multiple natural language processing tasks, and we focused on eight specific datasets for our evaluation. These datasets cover various aspects of language understanding and include the following tasks: sentiment classification (SST-2), paraphrase detection (MRPC and QQP), natural language inference (MNLI, RTE, and QNLI), linguistic acceptability (CoLA), and Semantic Textual Similarity (STS-B).

Additionally, we used the SQuAD dataset, which is a well-known reading comprehension benchmark. The SQuAD dataset consists of question-answering pairs, where the model is required to provide answers based on a given passage. More details about the datasets are provided in Appendix A.2.

Pretrained Language Models: We used pre-trained RoBERTa_{Large} (355M parameters, 24 layers) (Liu et al., 2019); BERT_{BASE} (110M parameters; 12 layers) (Devlin et al., 2019); T5_{SMALL} (60M parameters; 6 encoder and decoder layers), T5_{BASE} (220M parameters; 12 encoder and decoder layers) (Raffel et al., 2019) models; Flan-T5-xl (3B parameters; 24 encoder and decoder layers), Flan-T5-xxl (11B parameters; 24 encoder and decoder layers) (Chung et al., 2022) instruction-tuned models. We also provide additional results with other models, including OPT (Zhang et al., 2022), GPT2 (Radford et al., 2019a), and ViT (Dosovitskiy et al., 2020), in Appendix A.3. Models {BERT_{BASE}, T5_{SMALL}, T5_{BASE}, OPT} uses ReLU activations while the rest of the models utilize GeLU-based activation.

PEFT Modules: We used {Adapter, LoRA, Prefix-Tuning (Prefix-T), Prompt Tuning (Prompt-T)} for {BERT, RoBERTa} and {Adapter, LoRA, QLoRA} for T5 models. These PEFT modules serve as the baselines to be compared with our proposed DEFT method.

More detailed information about the hyperparameters employed in our experiments can be found in Appendix A.2.

Evaluation Metrics: To assess the performance of our proposed method DEFT and the baselines (PEFT) on the GLUE benchmark datasets, we utilize various evaluation metrics tailored to the specific tasks. For the Semantic Textual Similarity (STS-B) dataset, we report the Pearson correlation coefficient. For the CoLA dataset, we report the Matthews correlation coefficient. In the case of MNLI, we report the accuracy achieved on the matched validation set. For all other tasks within the GLUE benchmark, we report the accuracy metric. For the SQuAD dataset, we report two widely-used metrics: F1 score and Exact-Match score.

In addition to task-specific metrics, we extend our evaluation to include the effectiveness of our method in promoting activation sparsity. To quantify this, we calculate the **Density (%)** of activations. This is done by identifying the number of non-zero values in the intermediate activation matrices within the MLP block of each transformer layer. We then average these values across all layers and the entire validation set.

Furthermore, we introduce the Density Change (%) metric, inspired by the energy consumption ratio concept from Shumailov et al. (Shumailov et al., 2021). This metric is particularly insightful as it provides a comparative measure of sparsity induced by our method compared to the baseline. The Density Change (%) is computed as follows:

$$\text{Density Change (\%)} = \left(\frac{\text{Density}_{\text{PEFT}} - \text{Density}_{\text{DEFT}}}{\text{Density}_{\text{PEFT}}} \right) \times 100 \tag{8}$$

Here, $\text{Density}_{\text{PEFT}}$ and $\text{Density}_{\text{DEFT}}$ represent the density percentages for the Parameter-Efficient Fine-Tuning (PEFT) and our Density-Efficient Fine-Tuning (DEFT) methods, respectively. This formula effectively highlights the reduction in activation density achieved through our approach.

Energy Consumption Ratio: Activation sparsity can be directly leveraged on hardware with zero-skip operations like ASIC accelerators. Therefore, our method DEFT, which promotes sparser activation, is expected to result in higher energy savings on such hardware. We used the energy consumption ratio From (Lazzaro et al., 2023), defined as the ratio between the energy consumed while using the zero-skipping operation and when using standard operations (without zero-skip). We also report Energy Change(%), computed as the ratio of relative change between PEFT and DEFT energy ratio divided by PEFT energy ratio.

In our experiments, we report all of our results on 3 different random seeds.

Density Loss Hyperparameters: For our density loss we used $\beta = 20$ with tanh approximation Eq. (3) and $\epsilon = 1e-07$ with l_0 -approximation Eq. (4) and $\alpha = 1.0$. We also provide an ablation study for varying these parameters later in Section 4.4.

Computing Resources: Our experimental setups leveraged 1 RTX8000 with 48GB memory for RoBERTa_{Large}, BERT_{BASE} (ReLU) and T5_{small}; T5_{base} utilized 2 RTX8000 GPUs and Flan-T5 models utilized 4 A100s with 80GB memory.

4.1. Results on GLUE Benchmark

The performance comparison of different methods on the GLUE benchmark using the RoBERTa_{Large} model is presented in Table 1. It provides insights into the effects of activation sparsification techniques on both performance metrics and activation density in the intermediate layers of the Transformer MLP block with only a few trainable parameters.

Across all datasets, the fine-tuning methods Adapter, LoRA, Prefix-Tuning (Prefix-T), and Prompt-Tuning (Prompt-T) were evaluated using two methods: PEFT and DEFT. We observe that all DEFT methods, including Adapter, LoRA, Prefix-T, and Prompt-T, generally achieve comparable performance to PEFT, with only marginal differences in most cases while significantly reducing the activation density. The results reveal that all methods consistently achieve significantly lower activation density compared to PEFT.

Reduction in Activation Density: Adapter > LoRA > Prefix-T > Prompt-T. We observe in all the cases, our proposed method, DEFT, promotes activation sparsity with minimal or no effect on the downstream performance. The reductions in activation density range from 0.02% (Prompt-T, MRPC) to 55.57% (Adapter, SST-2) across the different datasets and methods. Notably, the method with the highest reduction in activation density on GLUE benchmark is Adapter (50.72%), followed by LoRA (38.82%) and Prefix-T (36.39%). Prompt-T shows the least reduction, at 1.44%, and specifically, we note a training collapse in the CoLA dataset using prompt-tuning. There is also one exception of the RTE dataset with Adapter module, where DEFT achieves lower performance than PEFT. As we discuss in Section 4.4, this can be mitigated by adjusting the weightage of the density loss term for specific datasets. It’s important to note that these results are not directly comparable across different modules due to variations in the number of trainable parameters and the location of additional parameters. For instance, prefix-tuning involves adding trainable

From PEFT to DEFT: Parameter Efficient Finetuning for Reducing Activation Density in Transformers

Table 1: Performance comparison on GLUE benchmarks with RoBERTa_{Large}. (*) denotes unstable training.

| Module (% Trainable) | Method | Performance | MNLI | QQP | QNLI | SST-2 | STS-B | MRPC | RTE | CoLA | Avg. |
|----------------------|--------|------------------------|------------|------------|------------|------------|-------------|-------------|------------|------------|--------------|
| Adapter (1.17%) | PEFT | Metric (↑) | 89.83±0.02 | 91.79±0.02 | 94.49±0.10 | 96.06±0.44 | 92.31±0.03 | 89.29±1.09 | 84.11±1.47 | 65.43±0.88 | 87.91 |
| | | Density (↓) | 94.24±0.02 | 94.06±0.05 | 94.23±0.02 | 93.83±0.12 | 94.41±0.02 | 94.32±0.08 | 94.54±0.06 | 94.19±0.06 | - |
| | DEFT | Metric (↑) | 89.76±0.20 | 91.32±0.07 | 93.67±0.23 | 96.17±0.35 | 91.76±0.43 | 74.42±8.72 | 50.42±1.62 | 67.14±1.77 | 81.83 |
| | | Density (↓) | 44.29±0.55 | 42.38±0.44 | 46.60±0.39 | 41.50±0.53 | 59.85±2.57 | 49.75±9.59 | 45.16±3.39 | 42.01±0.26 | - |
| | | Density Change (%) (↑) | 53.00 | 54.94 | 50.55 | 55.77 | 36.61 | 47.25 | 52.23 | 55.40 | 50.72 |
| LoRA (1.16%) | PEFT | Metric (↑) | 90.53±0.12 | 91.38±0.04 | 94.71±0.03 | 95.67±0.19 | 91.21±0.24 | 91.63±0.46 | 81.94±0.51 | 63.21±0.01 | 87.54 |
| | | Density (↓) | 94.61±0.01 | 94.35±0.15 | 94.49±0.05 | 93.87±0.13 | 94.32±0.03 | 94.28±0.13 | 94.50±0.03 | 94.18±0.06 | - |
| | DEFT | Metric (↑) | 90.27±0.21 | 90.79±0.23 | 93.89±0.21 | 95.99±0.33 | 91.52±0.16 | 85.11±4.81 | 81.40±1.98 | 61.33±0.94 | 86.29 |
| | | Density (↓) | 43.64±0.46 | 49.08±1.29 | 48.65±0.98 | 45.86±1.66 | 87.61±3.35 | 44.00±5.94 | 85.83±0.14 | 57.01±0.95 | - |
| | | Density Change (%) (↑) | 53.87 | 47.98 | 48.51 | 51.15 | 7.11 | 53.33 | 9.17 | 39.47 | 38.82 |
| Prefix-T (1.11%) | PEFT | Metric (↑) | 89.99±0.12 | 89.77±0.07 | 94.59±0.05 | 95.64±0.16 | 90.52±0.24 | 86.76±0.91 | 74.84±1.51 | 59.10±0.80 | 85.15 |
| | | Density (↓) | 94.88±0.08 | 94.31±0.21 | 94.14±0.23 | 94.20±0.24 | 94.24±0.15 | 93.87±0.18 | 94.14±0.03 | 93.73±0.27 | - |
| | DEFT | Metric (↑) | 89.89±0.03 | 89.53±0.12 | 94.40±0.06 | 95.72±0.05 | 90.58±0.08 | 87.66±0.41 | 71.60±1.51 | 61.35±1.46 | 85.09 |
| | | Density (↓) | 50.83±0.60 | 46.16±0.27 | 56.19±0.34 | 51.91±0.65 | 74.53±1.48 | 71.88±0.64 | 76.51±0.91 | 51.18±0.97 | - |
| | | Density Change (%) (↑) | 46.43 | 51.06 | 40.31 | 44.89 | 20.91 | 23.43 | 18.73 | 45.4 | 36.39 |
| Prompt-T (0.31%) | PEFT | Metric (↑) | 81.53±1.93 | 84.17±0.29 | 80.88±1.89 | 84.63±1.68 | 22.66±14.31 | 71.159±2.21 | 51.98±3.34 | 2.18±3.08* | 59.89 |
| | | Density (↓) | 93.78±0.11 | 93.74±0.15 | 93.10±0.92 | 93.64±0.03 | 93.77±0.01 | 93.67±0.02 | 93.82±0.02 | 93.55±0.12 | - |
| | DEFT | Metric (↑) | 81.86±1.09 | 83.93±0.39 | 81.34±2.35 | 84.51±1.07 | 24.67±14.11 | 71.07±2.03 | 51.98±2.84 | 0.00* | 59.92 |
| | | Density (↓) | 88.84±0.41 | 89.29±1.53 | 93.00±0.10 | 92.90±0.18 | 93.74±0.01 | 93.65±0.03 | 93.79±0.02 | 93.05±0.33 | - |
| | | Density Change (%) (↑) | 5.27 | 4.75 | 0.11 | 0.79 | 0.03 | 0.02 | 0.03 | 0.53 | 1.44 |

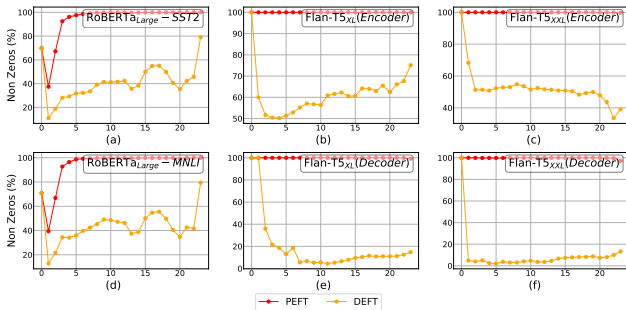


Figure 2: **Percentage of Non-zeros (density).** Layerwise non-zeros (%) for RoBERTa_{Large} (a,d), Flan-T5_{XL} (b,e) with Adapter module, and Flan-T5_{XXL} with QLoRA module on the validation set of different tasks. The x-axis is the layer index.

parameters to the hidden states. Nonetheless, the generality of DEFT is evident that all methods effectively promote activation sparsity with minimal impact on downstream performance in most cases.

Layerwise Activation Sparsity Analysis. To delve deeper into the effects of our method, we analyze layerwise activation sparsity in RoBERTa_{Large} when paired with the Adapter module. This analysis is visually represented in Fig. 2 for the SST-2 (a) and MNLI (d) datasets. Given that RoBERTa_{Large} comprises 24 layers, we computed the percentage of non-zero activations across these layers using the validation datasets. The resulting plots reveal a pronounced decrease in non-zero activations at each layer, underscoring DEFT’s efficiency in inducing activation sparsity throughout the network’s depth.

More Results for ReLU-Based Models. In this part of our study, we focus on the pre-trained BERT_{BASE} model, which employs ReLU activation functions. For our density loss calculations in Eq. (5), we utilize the tanh approximation in Eq. (3). We showcase the strength of our proposed method DEFT compared to PEFT in Figure (3a, 3b) for 8

Table 2: Energy Consumption Ratio with different models using ASIC Simulator developed in (Shumailov et al., 2021).

| Model | Method | ER | |
|-------------------------------------|--------|------------------|-------|
| RoBERTa _{Large} (Adapter) | PEFT | 0.85 | |
| | DEFT | 0.78 | |
| | | Energy Change(%) | 8.23% |
| RoBERTa _{Large} (LoRA) | PEFT | 0.84 | |
| | DEFT | 0.79 | |
| | | Energy Change(%) | 5.95% |
| RoBERTa _{Large} (Prefix-T) | PEFT | 0.90 | |
| | DEFT | 0.82 | |
| | | Energy Change(%) | 8.88% |
| RoBERTa _{Large} (Prompt-T) | PEFT | 0.898 | |
| | DEFT | 0.897 | |
| | | Energy Change(%) | 0.11% |
| Flan-T5 _{XL} (Adapter) | PEFT | 1.00 | |
| | DEFT | 0.87 | |
| | | Energy Change(%) | 13% |
| Flan-T5 _{XXL} (QLoRA) | PEFT | 1.00 | |
| | DEFT | 0.85 | |
| | | Energy Change(%) | 15% |

datasets from GLUE benchmark when adapting BERT_{BASE} model with the adapter module. Our proposed method, DEFT leads to sparser activation patterns compared to PEFT. In Figure (3a) we show the Density (%) in the intermediate output of MLP layers in transformer blocks averaged over the full validation dataset, and in (3b) we show the accuracy (%) on validation dataset, which shows that our method DEFT also maintains competitive performance with PEFT while reducing activation density. For a more comprehensive analysis, including detailed results of the BERT_{BASE} (ReLU) model with other modules, we refer the readers to Appendix A.3.2.

In Table 2, we report the energy consumption ratio and energy change (%). We used SST2 dataset from GLUE benchmark and reported our results on RoBERTa_{Large} with four modules. From the results, we can see that DEFT leads to a reduction in Energy Consumption compared to PEFT on the ASIC simulator.

It is worth noting that the impact of activation sparsity techniques varies across different datasets. For some datasets,

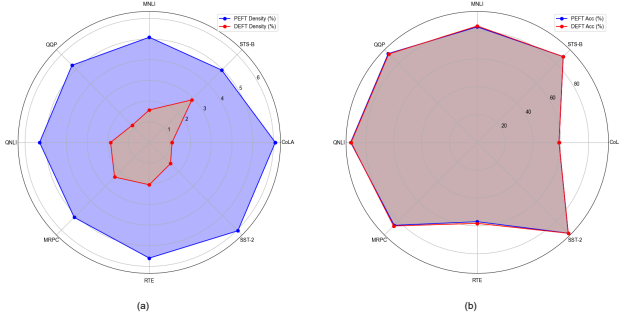


Figure 3: (a) Comparison of Activation Density (%) and (b) Accuracy (%) for GLUE benchmark datasets using BERT_{BASE} (ReLU) with Adapter for PEFT and DEFT.

the differences in performance metrics are minimal, indicating a similar impact from both PEFT and DEFT approaches. However, other datasets, like RTE, show a more pronounced disparity. Specifically, we observed a decrease in performance when applying DEFT with the Adapter module on the RTE dataset, as presented in Table 1. These results underscore the dataset-dependent nature of the density loss’s impact. While some datasets may be less sensitive to activation sparsity, others might exhibit more variability. In the subsequent ablation study in Section 4.4, we address these variations by fine-tuning the weightage given to the density loss. This adjustment demonstrates that carefully calibrating the density loss weight can effectively mitigate performance discrepancies and enhance the overall effectiveness of our DEFT method .

4.2. Results on SQuAD Dataset

Table 3 offers a comparative analysis of various methods applied to the SQuAD dataset using four T5 models. The evaluation focuses on two performance metrics: F1 score and Exact-Match, which measure the accuracy of the model’s answers. Additionally, the table provides information on the encoder and decoder activation densities. Note that, for our experiments, we introduce the density loss for both encoder and decoder layers with an equal weightage of 1.0. It is also possible to introduce the density loss for one of them. T5_{SMALL} and T5_{BASE} use ReLU activations while Flan-T5_{XL} and Flan-T5_{XXL} use GeLU based activation.

Results for ReLU-Based Models. For the ReLU-based models, we used tanh-approximation in Eq. (3) in the density loss as defined in Eq. (5). For the T5_{SMALL} model, the results indicate that both methods, namely PEFT and DEFT, achieve comparable performances, with only slight variations in the F1 score and Exact-Match metrics. As evident from the RoBERTa_{Large} experiments, the proposed method DEFT leads to a significant reduction in activation density for both encoder and decoder layers. The density change (%) for the encoder ranges from 26.26% to 30.62%, while for the decoder, they range from 52.08% to 61.96%

when compared to PEFT methods. For the T5_{BASE} model, the density reductions for the encoder range from 39.01% to 47.77%, while for the decoder, they range from 70.19% to 81.82%.

Larger models lead to more sparse activation patterns with DEFT. For Flan-T5 models which utilizes GeLU activations, we used the l_0 -approximation specified in Eq. (4) in the density loss of Eq. (5). We investigated our proposed method on larger instruction-tuned models, namely Flan-T5_{XL} (3B) and Flan-T5_{XXL} (11B). From the results, we can clearly see that our method consistently achieves a significant reduction in activation density for both encoder and decoder layers for larger models. For the Flan-T5_{XL} (3B) model with only 0.87% trainable parameters, we achieve density change (%) for the encoder 38.46%, while for the decoder, we achieve 81.29% when compared to PEFT methods. Similarly, for Flan-T5_{XXL} (11B) model, with only 0.52% trainable parameters, we achieve density change (%) of 53.19% for the encoder and 90.60% for Decoder compared to PEFT. These findings indicate that DEFT tends to induce sparser activation patterns as the model size increases, as summarized in Fig. (1b).

Layerwise Activation Sparsity Analysis. To provide further insights, we present layerwise non-zero (%) activation plots in Fig. 2 using Flan-T5 models on SQuAD dataset. Both models have 24 layers for both encoder and decoder. The plots distinctly show that DEFT significantly reduces the number of non-zero activations in both the encoder (b,c) and decoder (e,f) layers. A notable observation is the more pronounced reduction in non-zeros in the decoder layers as compared to the encoder layers. In these experiments, we employed a uniform weight of 1.0 for both the encoder and decoder density loss terms. However, optimizing the balance between encoder and decoder activation sparsity by assigning individual weights to their respective density loss terms presents an intriguing avenue for future research.

In Table 2, we report energy consumption ratio and energy change (%) for Flan-T5 models. We can see from the results that DEFT leads to a decrease in energy consumption, especially for Flan-T5_{XXL}, which demonstrates a noteworthy 15% decrease in energy consumption with DEFT compared to PEFT.

In summary, the results demonstrate that the Adapter and LoRA modules can maintain competitive performance on the SQuAD dataset while achieving notable reductions in activation density.

4.3. Pruning of PEFT/DEFT Models

In this section, we explore the effects of model pruning using the recently introduced WANDA metric (Sun et al., 2023b). The WANDA metric combines weight magnitude and activations to identify parameters for pruning.

Table 3: Performance comparison of different methods on Question Answering Dataset (SQuAD) with T5 models.

| Model | Module (% Trainable) | Loss Type | SQuAD | | | |
|---------------------------------|----------------------|-----------|--------------|--------------|--------------|--------------|
| | | | F1 | Exact-Match | Enc-Density | Dec-Density |
| T5- Small (60M) | Adapter (0.33%) | PEFT | 82.58 ± 0.08 | 74.48 ± 0.07 | 4.76 ± 0.01 | 4.07 ± 0.03 |
| | | DEFT | 82.41 ± 0.11 | 74.19 ± 0.13 | 3.51 ± 0.07 | 1.95 ± 0.01 |
| | Density Change(%) | | | 26.26 | 52.08 | |
| T5- Base (220M) | Adapter (0.40%) | PEFT | 88.28 ± 0.04 | 81.19 ± 0.05 | 2.64 ± 0.02 | 3.22 ± 0.04 |
| | | DEFT | 88.21 ± 0.04 | 81.08 ± 0.12 | 1.61 ± 0.03 | 0.96 ± 0.05 |
| | Density Change(%) | | | 39.01 | 70.19 | |
| Flan-T5 _{XL} (3B) | Adapter (0.87%) | PEFT | 92.81 ± 0.03 | 87.28 ± 0.13 | 99.99 ± 0.00 | 99.96 ± 0.00 |
| | | DEFT | 92.52 ± 0.03 | 86.79 ± 0.13 | 61.53 ± 0.05 | 18.70 ± 0.27 |
| | Density Change(%) | | | 38.46 | 81.29 | |
| Flan-T5 _{XXL} (11B) | QLoRA (0.52%) | PEFT | 92.84 ± 0.07 | 86.75 ± 0.07 | 99.97 ± 0.00 | 99.82 ± 0.01 |
| | | DEFT | 92.72 ± 0.15 | 87.04 ± 0.14 | 46.80 ± 5.65 | 9.38 ± 0.41 |
| | Density Change(%) | | | 53.19 | 90.60 | |

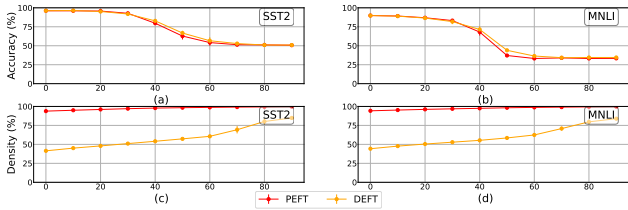


Figure 4: **Metric v.s. Sparsity.** Performance of RoBERTa_{Large} with Adapter for different pruning thresholds for MLP block using WANDA metric on the validation set. (a) and (c): Accuracy and Density (%) on SST2 dataset. (b) and (d): Accuracy and Density (%) on MNLI dataset.

Formally, given a weight matrix $W \in \mathbb{R}^{d_{out} \times d_{in}}$ and input activations $X \in \mathbb{R}^{N \times K \times d_{in}}$, where N is the batch size and K is the sequence length. The importance score of each weight is calculated by the product of weight magnitude and corresponding feature norm:

$$I_{ij} = |W_{ij}| \cdot \|X_j\|_2 \tag{9}$$

where $|\cdot|$ is the absolute value operator and $\|X_j\|_2$ is the l_2 averaged norm across the $N \times K$ tokens of the j th feature.

To perform pruning, we randomly select 128 samples from the training set of each respective downstream dataset and use the WANDA metric to identify the parameters in MLP blocks. Specifically, we prune the first dense layer in the MLP layer for all transformer blocks. The goal is to investigate the impact of sparsity induced by pruning on the model’s performance. We provide the results with the one where we first adapt the model using PEFT/DEFT and then prune using WANDA (adapt-prune) to downstream tasks. Fig. 4 showcases the performance of the pruned RoBERTa_{large} model, which was first adapted to the downstream datasets using both PEFT and DEFT with Adapter.

We report the performance on the validation dataset of SST-2 and MNLI. Fig. 4 reveals a notable pattern: when pruning after adapting to a downstream task, initially, as the sparsity level increases, the performance (measured in Accuracy) remains stable at lower levels of sparsity. However, beyond a certain threshold, a decline in performance is observed, eventually reaching a saturation point. Notably, DEFT exhibits either higher or comparable accuracy to PEFT across various sparsity levels while achieving greater activation sparsity. For example, as shown in Fig. 4 (b,d), at 40% sparsity, the model utilizing DEFT attains an accuracy of 71.45% with an activation Density of 55.33%, outperforming PEFT, which achieves only 68.06% accuracy with a significantly higher Density of 97.51%. This outcome suggests that DEFT can effectively complement weight pruning methods like WANDA, enabling models to benefit from both activation and weight sparsity.

4.4. Ablation Study

In this section, we perform an ablation study on two parameters used in our proposed method DEFT in Eq. (7): α (weight for the density loss) and ϵ (used in the l_0 approximation in Eq. (4)). For this study, we used the RoBERTa_{Large} model with the RTE and SST-2 datasets.

First, we investigate the impact of varying α on the accuracy and density. Fig. 5 presents the results, showing the accuracy (b) and density (d) for different values of α , while keeping ϵ fixed at $1e - 07$ on the RTE dataset. As we increase the weightage, we observe a decrease in density as the activations in the intermediate layer of the MLP become sparser. However, this increased sparsity comes at the cost of decreased accuracy. Hence, there is a trade-off between sparsity and downstream performance. Higher values of α lead to sparser activations but lower accuracy. Also, as

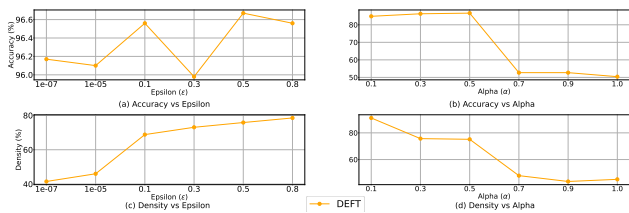


Figure 5: **Ablation Study.** Varying α and ϵ parameters using Adapter module with RoBERTa_{Large} on RTE and SST2 datasets, respectively.

discussed in Section 4.1, the adapter module with DEFT leads to lower accuracy for the RTE dataset, we can see that for the $\alpha = 0.50$ will lead to recovering accuracy to **86.64%** with density 75.16% while PEFT achieves **84.11%** with Density 94.54% from Table 1.

Next, we examine the impact of varying ϵ on the accuracy and density. Fig. 5 illustrates the results, displaying the accuracy (a) and density (c) for different values of ϵ , with α fixed at 1.0 on the SST2 dataset. As we increase ϵ , we observe a rapid increase in density initially, which then saturates. Notably, our method’s resilience remains evident as fluctuations in the ϵ parameter exhibit a minimal impact on the overall performance (accuracy).

These ablation studies shed light on the effects of α and ϵ on activation sparsity and downstream performance. By varying these parameters, we can control the trade-off between sparsity and accuracy, allowing for customization based on specific requirements and constraints.

5. Conclusion

In this work, we presented our method DEFT, a novel add-on module to PEFT for inducing activation sparsity in MLP layers of frozen pre-trained transformer blocks. We demonstrate the effectiveness of DEFT for reducing the activation density without hurting downstream performance compared to PEFT by various experiments on RoBERTa_{Large} and BERT_{BASE} with GLUE benchmark, {T5-Small, T5-Base, Flan-T5_{XL}, Flan-T5_{XXL}} on QA (SQuAD 1.0) benchmark, and with different parameter-efficient modules. Extensive experimental results confirm that our proposed DEFT provides new means for density-efficient PEFT of pretrained language models to improve inference efficiency while maintaining similar model performance. We also showcase the effect of pruning with the DEFT models and find that DEFT can be used as a complementary method with weight pruning methods, leading to both activation and weight sparsity. We believe that our proposed DEFT opens a new avenue for density-efficient fine-tuning of pre-trained models.

References

- Behnke, M. and Heafield, K. Losing heads in the lottery: Pruning transformer attention in neural machine translation. In Webber, B., Cohn, T., He, Y., and Liu, Y. (eds.), *Proceedings of the 2020 Conference on Empirical Methods in Natural Language Processing, EMNLP 2020, Online, November 16-20, 2020*, pp. 2664–2674. Association for Computational Linguistics, 2020. doi: 10.18653/v1/2020.emnlp-main.211. URL <https://doi.org/10.18653/v1/2020.emnlp-main.211>.
- Chen, X., Chen, T., Cheng, Y., Chen, W., Wang, Z., and Awadallah, A. H. DSEE: dually sparsity-embedded efficient tuning of pre-trained language models. *CoRR*, abs/2111.00160, 2021. URL <https://arxiv.org/abs/2111.00160>.
- Chung, H. W., Hou, L., Longpre, S., Zoph, B., Tay, Y., Fedus, W., Li, E., Wang, X., Dehghani, M., Brahma, S., Webson, A., Gu, S. S., Dai, Z., Suzgun, M., Chen, X., Chowdhery, A., Valter, D., Narang, S., Mishra, G., Yu, A. W., Zhao, V., Huang, Y., Dai, A. M., Yu, H., Petrov, S., hsin Chi, E. H., Dean, J., Devlin, J., Roberts, A., Zhou, D., Le, Q. V., and Wei, J. Scaling instruction-finetuned language models. *ArXiv*, abs/2210.11416, 2022. URL <https://api.semanticscholar.org/CorpusID:253018554>.
- Dettmers, T., Lewis, M., Belkada, Y., and Zettlemoyer, L. Llm.int8(): 8-bit matrix multiplication for transformers at scale. *CoRR*, abs/2208.07339, 2022. doi: 10.48550/arXiv.2208.07339. URL <https://doi.org/10.48550/arXiv.2208.07339>.
- Dettmers, T., Pagnoni, A., Holtzman, A., and Zettlemoyer, L. Qlora: Efficient finetuning of quantized llms. *ArXiv*, abs/2305.14314, 2023a. URL <https://api.semanticscholar.org/CorpusID:258841328>.
- Dettmers, T., Pagnoni, A., Holtzman, A., and Zettlemoyer, L. Qlora: Efficient finetuning of quantized llms. *CoRR*, abs/2305.14314, 2023b. doi: 10.48550/ARXIV.2305.14314. URL <https://doi.org/10.48550/arXiv.2305.14314>.
- Devlin, J., Chang, M.-W., Lee, K., and Toutanova, K. Bert: Pre-training of deep bidirectional transformers for language understanding. *ArXiv*, abs/1810.04805, 2019.
- Dosovitskiy, A., Beyer, L., Kolesnikov, A., Weissenborn, D., Zhai, X., Unterthiner, T., Dehghani, M., Minderer, M., Heigold, G., Gelly, S., Uszkoreit, J., and Houlsby, N. An image is worth 16x16 words: Transformers for image recognition at scale. *ArXiv*, abs/2010.11929, 2020. URL <https://api.semanticscholar.org/CorpusID:225039882>.

- Hendrycks, D. and Gimpel, K. Gaussian error linear units (gelus). *arXiv: Learning*, 2016. URL <https://api.semanticscholar.org/CorpusID:125617073>.
- Houlsby, N., Giurghi, A., Jastrzebski, S., Morrone, B., de Laroussilhe, Q., Gesmundo, A., Attariyan, M., and Gelly, S. Parameter-efficient transfer learning for NLP. In Chaudhuri, K. and Salakhutdinov, R. (eds.), *Proceedings of the 36th International Conference on Machine Learning, ICML 2019, 9-15 June 2019, Long Beach, California, USA*, volume 97 of *Proceedings of Machine Learning Research*, pp. 2790–2799. PMLR, 2019. URL <http://proceedings.mlr.press/v97/houlsby19a.html>.
- Howard, J. and Ruder, S. Universal language model finetuning for text classification. In Gurevych, I. and Miyao, Y. (eds.), *Proceedings of the 56th Annual Meeting of the Association for Computational Linguistics, ACL 2018, Melbourne, Australia, July 15-20, 2018, Volume 1: Long Papers*, pp. 328–339. Association for Computational Linguistics, 2018. doi: 10.18653/v1/P18-1031. URL <https://aclanthology.org/P18-1031/>.
- Hu, E. J., Shen, Y., Wallis, P., Allen-Zhu, Z., Li, Y., Wang, S., Wang, L., and Chen, W. Lora: Low-rank adaptation of large language models. In *The Tenth International Conference on Learning Representations, ICLR 2022, Virtual Event, April 25-29, 2022*. OpenReview.net, 2022. URL <https://openreview.net/forum?id=nZeVKeeFYf9>.
- Krithivasan, S., Sen, S., and Raghunathan, A. Adversarial sparsity attacks on deep neural networks. *ArXiv*, abs/2006.08020, 2020.
- Krizhevsky, A., Hinton, G., et al. Learning multiple layers of features from tiny images. 2009.
- Kudugunta, S., Huang, Y., Bapna, A., Krikun, M., Lepikhin, D., Luong, M., and Firat, O. Beyond distillation: Task-level mixture-of-experts for efficient inference. In Moens, M., Huang, X., Specia, L., and Yih, S. W. (eds.), *Findings of the Association for Computational Linguistics: EMNLP 2021, Virtual Event / Punta Cana, Dominican Republic, 16-20 November, 2021*, pp. 3577–3599. Association for Computational Linguistics, 2021. doi: 10.18653/v1/2021.findings-emnlp.304. URL <https://doi.org/10.18653/v1/2021.findings-emnlp.304>.
- Kurtz, M., Kopinsky, J., Gelashvili, R., Matveev, A., Carr, J., Goin, M., Leiserson, W. M., Moore, S., Shavit, N., and Alistarh, D. Inducing and exploiting activation sparsity for fast inference on deep neural networks. In *Proceedings of the 37th International Conference on Machine Learning, ICML 2020, 13-18 July 2020, Virtual Event*, volume 119 of *Proceedings of Machine Learning Research*, pp. 5533–5543. PMLR, 2020. URL <http://proceedings.mlr.press/v119/kurtz20a.html>.
- Lazzaro, D., Cinà, A. E., Pintor, M., Demontis, A., Biggio, B., Roli, F., and Pelillo, M. Minimizing energy consumption of deep learning models by energy-aware training. *arXiv preprint arXiv:2307.00368*, 2023.
- Lee, N., Ajanthan, T., and Torr, P. H. S. Snip: single-shot network pruning based on connection sensitivity. In *7th International Conference on Learning Representations, ICLR 2019, New Orleans, LA, USA, May 6-9, 2019*. OpenReview.net, 2019. URL <https://openreview.net/forum?id=B1VZqjAcYX>.
- Lester, B., Al-Rfou, R., and Constant, N. The power of scale for parameter-efficient prompt tuning. In Moens, M., Huang, X., Specia, L., and Yih, S. W. (eds.), *Proceedings of the 2021 Conference on Empirical Methods in Natural Language Processing, EMNLP 2021, Virtual Event / Punta Cana, Dominican Republic, 7-11 November, 2021*, pp. 3045–3059. Association for Computational Linguistics, 2021. doi: 10.18653/v1/2021.emnlp-main.243. URL <https://doi.org/10.18653/v1/2021.emnlp-main.243>.
- Li, J., Cotterell, R., and Sachan, M. Differentiable subset pruning of transformer heads. *Trans. Assoc. Comput. Linguistics*, 9:1442–1459, 2021. doi: 10.1162/tacl_a_00436. URL https://doi.org/10.1162/tacl_a_00436.
- Li, X. L. and Liang, P. Prefix-tuning: Optimizing continuous prompts for generation. In Zong, C., Xia, F., Li, W., and Navigli, R. (eds.), *Proceedings of the 59th Annual Meeting of the Association for Computational Linguistics and the 11th International Joint Conference on Natural Language Processing, ACL/IJCNLP 2021, (Volume 1: Long Papers), Virtual Event, August 1-6, 2021*, pp. 4582–4597. Association for Computational Linguistics, 2021. doi: 10.18653/v1/2021.acl-long.353. URL <https://doi.org/10.18653/v1/2021.acl-long.353>.
- Li, Z., You, C., Bhojanapalli, S., Li, D., Rawat, A. S., Reddi, S. J., Ye, K., Chern, F., Yu, F. X., Guo, R., and Kumar, S. Large models are parsimonious learners: Activation sparsity in trained transformers. *CoRR*, abs/2210.06313, 2022. doi: 10.48550/arXiv.2210.06313. URL <https://doi.org/10.48550/arXiv.2210.06313>.
- Liu, Y., Ott, M., Goyal, N., Du, J., Joshi, M., Chen, D., Levy, O., Lewis, M., Zettlemoyer, L., and Stoyanov, V. Roberta: A robustly optimized bert pretraining approach. *ArXiv*, abs/1907.11692, 2019. URL <https://api.semanticscholar.org/CorpusID:198953378>.
- Loshchilov, I. and Hutter, F. Fixing weight decay regularization in adam. *ArXiv*, abs/1711.05101, 2017.

- Mangrulkar, S., Gugger, S., Debut, L., Belkada, Y., and Paul, S. Peft: State-of-the-art parameter-efficient finetuning methods. <https://github.com/huggingface/peft>, 2022.
- Michel, P., Levy, O., and Neubig, G. Are sixteen heads really better than one? In Wallach, H. M., Larochelle, H., Beygelzimer, A., d’Alché-Buc, F., Fox, E. B., and Garnett, R. (eds.), *Advances in Neural Information Processing Systems 32: Annual Conference on Neural Information Processing Systems 2019, NeurIPS 2019, December 8-14, 2019, Vancouver, BC, Canada*, pp. 14014–14024, 2019. URL <https://proceedings.neurips.cc/paper/2019/hash/2c601ad9d2ff9bc8b282670cdd54f69f-Abstract.html>.
- Pfeiffer, J., Rücklé, A., Poth, C., Kamath, A., Vulić, I., Ruder, S., Cho, K., and Gurevych, I. AdapterHub: A framework for adapting transformers. In *Proceedings of the 2020 Conference on Empirical Methods in Natural Language Processing: System Demonstrations*, pp. 46–54, Online, October 2020a. Association for Computational Linguistics. doi: 10.18653/v1/2020.emnlp-demos.7. URL <https://aclanthology.org/2020.emnlp-demos.7>.
- Pfeiffer, J., Vulić, I., Gurevych, I., and Ruder, S. MAD-X: An Adapter-Based Framework for Multi-Task Cross-Lingual Transfer. In *Proceedings of the 2020 Conference on Empirical Methods in Natural Language Processing (EMNLP)*, pp. 7654–7673, Online, November 2020b. Association for Computational Linguistics. doi: 10.18653/v1/2020.emnlp-main.617. URL <https://aclanthology.org/2020.emnlp-main.617>.
- Radford, A., Wu, J., Child, R., Luan, D., Amodei, D., and Sutskever, I. Language models are unsupervised multitask learners. 2019a. URL <https://api.semanticscholar.org/CorpusID:160025533>.
- Radford, A., Wu, J., Child, R., Luan, D., Amodei, D., and Sutskever, I. Language models are unsupervised multitask learners. 2019b. URL https://d4mucfpksywv.cloudfront.net/better-language-models/language_models_are_unsupervised_multitask_learners.pdf.
- Raffel, C., Shazeer, N. M., Roberts, A., Lee, K., Narang, S., Matena, M., Zhou, Y., Li, W., and Liu, P. J. Exploring the limits of transfer learning with a unified text-to-text transformer. *ArXiv*, abs/1910.10683, 2019.
- Raffel, C., Shazeer, N., Roberts, A., Lee, K., Narang, S., Matena, M., Zhou, Y., Li, W., and Liu, P. J. Exploring the limits of transfer learning with a unified text-to-text transformer. *J. Mach. Learn. Res.*, 21:140:1–140:67, 2020. URL <http://jmlr.org/papers/v21/20-074.html>.
- Rajbhandari, S., Li, C., Yao, Z., Zhang, M., Aminabadi, R. Y., Awan, A. A., Rasley, J., and He, Y. Deepspeed-moe: Advancing mixture-of-experts inference and training to power next-generation AI scale. In Chaudhuri, K., Jegelka, S., Song, L., Szepesvári, C., Niu, G., and Sabato, S. (eds.), *International Conference on Machine Learning, ICML 2022, 17-23 July 2022, Baltimore, Maryland, USA*, volume 162 of *Proceedings of Machine Learning Research*, pp. 18332–18346. PMLR, 2022. URL <https://proceedings.mlr.press/v162/rajbhandari22a.html>.
- Rajpurkar, P., Zhang, J., Lopyrev, K., and Liang, P. Squad: 100,000+ questions for machine comprehension of text. *ArXiv*, abs/1606.05250, 2016.
- Sanh, V., Debut, L., Chaumond, J., and Wolf, T. Distilbert, a distilled version of BERT: smaller, faster, cheaper and lighter. *CoRR*, abs/1910.01108, 2019. URL <http://arxiv.org/abs/1910.01108>.
- Shumailov, I., Zhao, Y., Bates, D., Papernot, N., Mullins, R., and Anderson, R. Sponge examples: Energy-latency attacks on neural networks. In *2021 IEEE European symposium on security and privacy (EuroS&P)*, pp. 212–231. IEEE, 2021.
- Strubell, E., Ganesh, A., and McCallum, A. Energy and policy considerations for deep learning in NLP. In Korhonen, A., Traum, D. R., and Márquez, L. (eds.), *Proceedings of the 57th Conference of the Association for Computational Linguistics, ACL 2019, Florence, Italy, July 28- August 2, 2019, Volume 1: Long Papers*, pp. 3645–3650. Association for Computational Linguistics, 2019. doi: 10.18653/v1/p19-1355. URL <https://doi.org/10.18653/v1/p19-1355>.
- Sun, M., Liu, Z., Bair, A., and Kolter, J. Z. A simple and effective pruning approach for large language models. *CoRR*, abs/2306.11695, 2023a. doi: 10.48550/arXiv.2306.11695. URL <https://doi.org/10.48550/arXiv.2306.11695>.
- Sun, M., Liu, Z., Bair, A., and Kolter, J. Z. A simple and effective pruning approach for large language models, 2023b.
- Tanaka, H., Kunin, D., Yamins, D. L. K., and Ganguli, S. Pruning neural networks without any data by iteratively conserving synaptic flow. In Larochelle, H., Ranzato, M., Hadsell, R., Balcan, M., and Lin, H. (eds.), *Advances in Neural Information Processing*

- Systems 33: Annual Conference on Neural Information Processing Systems 2020, NeurIPS 2020, December 6-12, 2020, virtual, 2020.* URL <https://proceedings.neurips.cc/paper/2020/hash/46a4378f835dc8040c8057beb6a2da52-Abstract.html>.
- Voita, E., Talbot, D., Moiseev, F., Sennrich, R., and Titov, I. Analyzing multi-head self-attention: Specialized heads do the heavy lifting, the rest can be pruned. In Korhonen, A., Traum, D. R., and Màrquez, L. (eds.), *Proceedings of the 57th Conference of the Association for Computational Linguistics, ACL 2019, Florence, Italy, July 28- August 2, 2019, Volume 1: Long Papers*, pp. 5797–5808. Association for Computational Linguistics, 2019. doi: 10.18653/v1/p19-1580. URL <https://doi.org/10.18653/v1/p19-1580>.
- Wang, A., Singh, A., Michael, J., Hill, F., Levy, O., and Bowman, S. GLUE: A multi-task benchmark and analysis platform for natural language understanding. In *Proceedings of the 2018 EMNLP Workshop BlackboxNLP: Analyzing and Interpreting Neural Networks for NLP*, pp. 353–355, Brussels, Belgium, November 2018. Association for Computational Linguistics. doi: 10.18653/v1/W18-5446. URL <https://aclanthology.org/W18-5446>.
- Wang, C., Zhang, G., and Grosse, R. B. Picking winning tickets before training by preserving gradient flow. In *8th International Conference on Learning Representations, ICLR 2020, Addis Ababa, Ethiopia, April 26-30, 2020*. OpenReview.net, 2020. URL <https://openreview.net/forum?id=SkgsACVKPH>.
- Wolf, T., Debut, L., Sanh, V., Chaumond, J., Delangue, C., Moi, A., Cistac, P., Rault, T., Louf, R., Funtowicz, M., Davison, J., Shleifer, S., von Platen, P., Ma, C., Jernite, Y., Plu, J., Xu, C., Le Scao, T., Gugger, S., Drame, M., Lhoest, Q., and Rush, A. Transformers: State-of-the-art natural language processing. In *Proceedings of the 2020 Conference on Empirical Methods in Natural Language Processing: System Demonstrations*, pp. 38–45, Online, October 2020. Association for Computational Linguistics. doi: 10.18653/v1/2020.emnlp-demos.6. URL <https://aclanthology.org/2020.emnlp-demos.6>.
- Zadeh, A. H., Edo, I., Awad, O. M., and Moshovos, A. GOBO: quantizing attention-based NLP models for low latency and energy efficient inference. In *53rd Annual IEEE/ACM International Symposium on Microarchitecture, MICRO 2020, Athens, Greece, October 17-21, 2020*, pp. 811–824. IEEE, 2020. doi: 10.1109/MICRO50266.2020.00071. URL <https://doi.org/10.1109/MICRO50266.2020.00071>.
- Zhang, S., Roller, S., Goyal, N., Artetxe, M., Chen, M., Chen, S., Dewan, C., Diab, M. T., Li, X., Lin, X. V., Mihaylov, T., Ott, M., Shleifer, S., Shuster, K., Simig, D., Koura, P. S., Sridhar, A., Wang, T., and Zettlemoyer, L. Opt: Open pre-trained transformer language models. *ArXiv*, abs/2205.01068, 2022. URL <https://api.semanticscholar.org/CorpusID:248496292>.
- Zhang, Z., Lin, Y., Liu, Z., Li, P., Sun, M., and Zhou, J. Moefication: Transformer feed-forward layers are mixtures of experts. In *Findings*, 2021.

A. Appendix

This section provides supplementary information encompassing dataset specifics, code for our experiments and Hyperparameter details for training. We provide more information regard Parameter-Efficient-Fine-Tuning (PEFT) in Section A.1; We provide an overview of dataset statistics in Section A.2. In section A.3.1, we delve into supplementary experiments exploring alternative avenues for approximating non-zero activation values. In Section A.3.3, we present additional experiments with Decoder only models and in Section A.3.4 on the image classification task. Finally, in Section ??, we present the energy consumption ratio on different models using ASIC simulator. Note that all the results reported are averaged across 3 random seeds.

A.1. Parameter Efficient Fine-Tuning Methods

Prompt tuning (Lester et al., 2021): Prompt tuning introduces additional trainable parameters called prompt embeddings or soft prompts. A soft prompt is comprised of trainable parameters Φ , that are prepended to the embedding of the input tokens for each datapoint. $\Phi \in \mathbb{R}^{P \times d_{\text{model}}}$, where P is length of soft prompt and d_{model} is the dimension of the model’s embeddings. The soft prompts are initialized randomly and are learnt end-to-end. Our input X in (1) would now become $X = \text{concat}([\Phi, \text{emb}(\text{input})])$. The soft prompt is the same for all the datapoints in a given downstream task. During training, the entire model’s parameters are frozen and only the prompt embeddings are updated during the backpropagation.

Prefix tuning (Li & Liang, 2021): In the case of prefix tuning, the trainable prompt embeddings are added to the input at each transformer layer rather than only at the beginning. The prefix tuning embeddings is now $\Phi \in \mathbb{R}^{L \times P \times d_{\text{model}}}$, where L is the number of transformer layers, P is the length of soft prompt, and d_{model} is the dimension of the model’s embeddings.

Adapters (Houlsby et al., 2019): The bottleneck adapters consist of a specialized feed-forward layer inserted within each transformer layer. The adapter architecture typically comprises a down-projection layer, a non-linear activation function, and an up-projection layer.

$$\text{Adapter} = U_{\text{MLP}}(\Omega(D_{\text{MLP}}(\text{inp}))) \tag{10}$$

where $U_{\text{MLP}} \in \mathbb{R}^{I \times m}$, $D_{\text{MLP}} \in \mathbb{R}^{m \times I}$. I is the dimension of the output of the feedback block, m is the dimension of the downward project, and $m \ll I$. The specific location of adapters within the transformer block can vary. In this work, we adopted the placement strategy from (Pfeiffer et al., 2020b), where the bottleneck layer is introduced only after each feedforward block in the transformer.

Low-Rank Adaptation (LORA) (Hu et al., 2022): During regular fine-tuning, the weights are updated using $W + \Delta W$. In LORA, during the update the model weights W are fixed, ΔW is decomposed to two lower rank matrices W_A and W_B , and these two matrices are learnt during the training. $W_A \in \mathbb{R}^{A \times r}$ and $W_B \in \mathbb{R}^{r \times B}$. To save the weights of the model fine-tuned on a new task, only these W_A and W_B matrices are saved and the final weights are obtained by pre-trained weights $W + W_A W_B$.

Quantized Low-Rank Adaptation (QLORA) (Detmeters et al., 2023b): The memory requirement for all the techniques described so far is comparable to that of fine-tuning. To address this, QLoRa extended LORA where the weights of the model are quantized using double quantization to 4bit NormalFloat.

A.2. Datasets, Code and Hyperparameters

We provide the statistics of the data in table 4. We provide the code for running our experiments in a zip file with the submission.

Training Details: For training the $\{\text{RoBERTa}_{\text{Large}}, \text{BERT}_{\text{BASE}}\}$ with adapter and LoRA modules, we used learning rate $lr = 3e - 4$, for prefix tuning we used $lr = 1e - 2$ and for prompt tuning, we used $lr = 1e - 3$. For all T5 models, we used $lr = 3e - 5$ for both adapter and LoRA modules. For parameter-efficient fine-tuning on downstream tasks, we freeze the parameters of the pre-trained models and we used 10 epochs with AdamW (Loshchilov & Hutter, 2017) with Batch size 64. For QLoRa with Flan-T5_{XXL}, we use 4-bit NF4 QLoRa with double quantization and paged optimizer(AdamW-32 bit) (Detmeters et al., 2023a) with Batch size of 4.

Parameter-Efficient Modules: For the Adapter, we added an adapter block after the feed-forward layer in each transformer block, following (Pfeiffer et al., 2020b). Specifically, we used a reduction factor of 16 for the BERT, RoBERTa and Flan-T5 models and 32 for the T5 models. For LoRA we used rank $r = 8$, $\alpha = 16$, dropout = 0.10 for BERT model and rank $r = 16$, $\alpha = 32$, dropout = 0.05 for T5 models and dropout = 0.10 for Flan-T5 models. For prefix and prompt tuning, we used 60 virtual tokens. We leveraged the PyTorch implementation of Adapter-transformers (Pfeiffer et al., 2020a) and the PEFT (Mangrulkar et al., 2022) library, which is built on the Hugging Face Transformers (Wolf et al., 2020) framework.

Table 4: Number of classes, Number of instances in Train and Validation split in datasets.

| Dataset | #Classes | #Train | #Validation |
|---------|----------|---------|-------------|
| COLA | 2 | 8550 | 1040 |
| MNLI | 3 | 393,000 | 19650 |
| MRPC | 2 | 3,670 | 408 |
| QNLI | 2 | 105,000 | 5,460 |
| QQP | 2 | 364,000 | 40,400 |
| RTE | 2 | 2,490 | 277 |
| SST2 | 2 | 67,300 | 872 |
| STS-B | - | 5,750 | 1,500 |
| SQuAD | - | 87,600 | 10,600 |

A.3. Experiments

A.3.1. APPROXIMATION OF NON-ZERO ACTIVATIONS

$\tanh > l_0 > \text{sigmoid} > l_1$. We compared DEFT with different approximations in Table 6. We found that among the four of them; the \tanh approximation works best for the ReLU-based model. Other approximation sigmoid and l_0 also performed well, however l_1 norm fails to retain good performance while reducing activation density, highlighting that a naive approximation of the activation matrix can lead to unstable training.

A.3.2. RESULTS ON GLUE BENCHMARK WITH BERT_{BASE} (ReLU)

We provide the results on GLUE benchmark in Table 5 on BERT_{BASE} (ReLU) model with different PEFT modules. We observe that all DEFT methods, including Adapter, LoRA, Prefix-T, and Prompt-T, generally achieve comparable performance to PEFT, with only marginal differences in most cases while significantly reducing the activation density. The results reveal that all methods consistently achieve significantly lower activation density compared to PEFT. We observe in all the cases, our proposed method DEFT promotes activation sparsity with minimal or no effect on the downstream performance. The reductions in activation density range from 2.66% (Prompt-T, STS-B) to 94.20% (LoRA, RTE) across the different datasets and methods. Notably, the method with the highest reduction in activation density on GLUE benchmark is Prefix-T (81.44%), followed by LoRA (77.41%) and Adapter (66.01%). Prompt-T achieves the lowest reduction among the methods (32.28%).

A.3.3. EXPERIMENTS WITH DECODER ONLY MODELS

We additionally tested our method with Decoder only models {OPT, GPT2} in Table 8. We used SST-2 dataset from GLUE. For GPT2, we used an adapter with reduction factor 8 for our experiments and for OPT models, we used LoRA with rank $r = 8$.

From the results, we can see that even for Decoder-only models, our method leads to a significant reduction in activation density both for OPT and GPT2 models.

A.3.4. EXPERIMENTS ON IMAGE CLASSIFICATION TASK

We tested the image classification task with ViT model (Dosovitskiy et al., 2020) on CIFAR-10 (Krizhevsky et al., 2009) dataset. For ViT, we used an adapter with a reduction factor of 8 for our experiments. For the CIFAR-10, we report the accuracy on the Test set containing 10k images.

From the results in Table 8, we can see that DEFT leads to reduction in activation density; for example, in ViT_{Large}, we see

From PEFT to DEFT: Parameter Efficient Finetuning for Reducing Activation Density in Transformers

Table 5: Performance comparison on GLUE benchmarks with BERT_{BASE} (ReLU).

| Module (% Trainable) | Method | Performance | MNLI | QQP | QNLI | SST-2 | STS-B | MRPC | RTE | CoLA | Avg. |
|----------------------|--------|------------------------|--------------|--------------|--------------|--------------|--------------|--------------|--------------|---------------|-------|
| Adapter (1.33%) | PEFT | Metric (↑) | 83.05 ± 0.89 | 90.28 ± 0.15 | 90.84 ± 0.10 | 92.27 ± 0.37 | 87.19 ± 0.34 | 84.26 ± 0.50 | 56.97 ± 1.79 | 58.65 ± 1.94 | 80.44 |
| | | Density (↓) | 5.09 ± 0.05 | 5.28 ± 0.11 | 5.30 ± 0.07 | 6.05 ± 0.15 | 4.95 ± 0.12 | 5.13 ± 0.09 | 5.60 ± 0.35 | 6.09 ± 0.11 | - |
| | DEFT | Metric (↑) | 83.68 ± 0.19 | 89.84 ± 0.25 | 90.50 ± 0.11 | 92.36 ± 0.36 | 87.17 ± 0.24 | 84.95 ± 0.59 | 58.19 ± 1.34 | 58.68 ± 0.93 | 80.67 |
| | | Density (↓) | 1.57 ± 0.02 | 1.17 ± 0.02 | 1.87 ± 0.03 | 1.45 ± 0.06 | 2.91 ± 0.18 | 2.37 ± 0.04 | 2.05 ± 0.13 | 1.10 ± 0.03 | - |
| | | Density Change (%) (↑) | 69.15 | 77.84 | 64.72 | 76.03 | 41.21 | 53.80 | 63.39 | 81.93 | 66.01 |
| LoRA (0.27%) | PEFT | Metric (↑) | 82.38 ± 0.46 | 89.09 ± 0.39 | 90.77 ± 0.18 | 92.48 ± 0.38 | 86.76 ± 0.44 | 86.52 ± 0.90 | 58.84 ± 1.00 | 55.86 ± 0.64 | 80.34 |
| | | Density (↓) | 5.44 ± 0.11 | 5.39 ± 0.12 | 5.86 ± 0.08 | 6.36 ± 0.21 | 5.57 ± 0.50 | 5.29 ± 0.38 | 5.86 ± 0.17 | 6.51 ± 1.32 | - |
| | DEFT | Metric (↑) | 81.83 ± 0.71 | 88.98 ± 0.49 | 90.64 ± 0.13 | 92.34 ± 0.26 | 86.98 ± 0.30 | 85.78 ± 0.73 | 53.94 ± 1.61 | 56.13 ± 0.85 | 79.58 |
| | | Density (↓) | 1.10 ± 0.10 | 0.78 ± 0.03 | 1.52 ± 0.01 | 1.03 ± 0.03 | 2.99 ± 0.19 | 1.70 ± 0.06 | 0.34 ± 0.32 | 0.8 ± 0.03 | - |
| | | Density Change (%) (↑) | 79.78 | 85.53 | 74.06 | 83.80 | 46.32 | 67.86 | 94.20 | 87.71 | 77.41 |
| Prefix-T (0.83%) | PEFT | Metric (↑) | 81.57 ± 0.58 | 87.99 ± 0.93 | 90.32 ± 0.14 | 92.29 ± 0.17 | 86.42 ± 0.40 | 84.66 ± 1.23 | 59.42 ± 1.44 | 56.47 ± 1.72 | 79.89 |
| | | Density (↓) | 5.98 ± 0.51 | 4.61 ± 0.27 | 5.21 ± 0.17 | 5.97 ± 0.72 | 4.91 ± 0.46 | 5.45 ± 0.29 | 6.18 ± 0.11 | 7.24 ± 1.32 | - |
| | DEFT | Metric (↑) | 81.11 ± 1.45 | 87.99 ± 0.84 | 89.84 ± 0.17 | 92.20 ± 0.26 | 86.62 ± 0.35 | 84.12 ± 1.55 | 54.01 ± 2.26 | 56.18 ± 1.41 | 79.01 |
| | | Density (↓) | 1.05 ± 0.09 | 0.71 ± 0.07 | 1.23 ± 0.04 | 1.02 ± 0.02 | 1.33 ± 0.08 | 1.51 ± 0.01 | 0.77 ± 0.45 | 0.52 ± 0.02 | - |
| | | Density Change (%) (↑) | 82.11 | 84.60 | 76.39 | 82.91 | 72.91 | 72.29 | 87.54 | 92.81 | 81.44 |
| Prompt-T (0.03%) | PEFT | Metric (↑) | 71.18 ± 1.14 | 80.15 ± 0.18 | 80.27 ± 1.08 | 86.51 ± 0.34 | 32.66 ± 8.41 | 70.29 ± 1.38 | 56.97 ± 1.64 | 13.68 ± 14.03 | 61.46 |
| | | Density (↓) | 4.39 ± 0.15 | 4.34 ± 0.11 | 4.10 ± 0.14 | 4.88 ± 0.11 | 4.14 ± 0.16 | 4.22 ± 0.05 | 4.40 ± 0.06 | 3.77 ± 0.13 | - |
| | DEFT | Metric (↑) | 71.01 ± 1.13 | 80.16 ± 0.42 | 80.37 ± 0.79 | 86.40 ± 0.36 | 32.77 ± 8.74 | 70.05 ± 1.34 | 57.26 ± 2.01 | 13.97 ± 13.41 | 61.50 |
| | | Density (↓) | 1.91 ± 0.01 | 1.53 ± 0.05 | 2.84 ± 0.24 | 2.18 ± 0.30 | 4.03 ± 0.14 | 3.95 ± 0.12 | 4.19 ± 0.07 | 2.37 ± 0.25 | - |
| | | Density Change (%) (↑) | 56.49 | 64.75 | 30.73 | 55.33 | 2.66 | 6.40 | 4.77 | 37.13 | 32.28 |

Table 6: Performance comparison with different approximations using BERT_{BASE} (ReLU) with Adapter module (1.33% trainable parameters).

| Method | Performance | SST2 |
|----------------|-------------|--------------|
| PEFT | Metric (↑) | 92.27 ± 0.37 |
| | Density (↓) | 6.05 ± 0.15 |
| DEFT (l_0) | Metric (↑) | 92.13 ± 0.30 |
| | Density (↓) | 1.41 ± 0.04 |
| DEFT (tanh) | Metric (↑) | 92.36 ± 0.36 |
| | Density (↓) | 1.45 ± 0.06 |
| DEFT (sigmoid) | Metric (↑) | 92.02 ± 0.05 |
| | Density (↓) | 1.51 ± 0.01 |
| DEFT (l_1) | Metric (↑) | 50.91 ± 0.00 |
| | Density (↓) | 0.50 ± 0.00 |

Table 7: Hyperparameters of different models used for additional study

| Models | Batch Size | lr |
|----------------------|------------|------|
| ViT _{Base} | 64 | 2e-5 |
| ViT _{Large} | 32 | 2e-5 |
| GPT2 | 32 | 3e-4 |
| OPT | 32 | 3e-4 |

DEFT achieves activation density of 70.33% while PEFT’s density is quite high 99.91%.

Table 8: Performance Comparison on different models with PEFT and DEFT.

| Method | Performance | ViT _{Base} (86M) | ViT _{Large} (307M) | OPT (125M) | OPT (350M) | GPT2 (117M) |
|------------------------|---------------|---------------------------|-----------------------------|------------|------------|--------------|
| | Trainable (%) | (2.04%) | (2.04%) | (0.24%) | (0.24%) | (1.87%) |
| PEFT | Metric (↑) | 98.13 ± 0.03 | 99.04 ± 0.06 | 91.50±0.11 | 93.34±0.46 | 88.38 ± 0.19 |
| | Density (↓) | 84.84 ± 0.09 | 99.91 ± 0.00 | 7.80±0.26 | 8.45±0.14 | 99.96 ± 0.00 |
| DEFT | Metric (↑) | 97.75 ± 0.09 | 98.31 ± 0.08 | 91.86±0.11 | 92.15±0.51 | 88.34 ± 0.39 |
| | Density (↓) | 77.74 ± 0.09 | 70.33 ± 2.47 | 1.24±0.002 | 1.87±0.01 | 70.51 ± 1.15 |
| Density Change (%) (↑) | | 8.38 | 29.61 | 84.10 | 77.87 | 29.46 |